



Excitable Patterns in Active Nematics

Citation

Giomi, Luca, Lakshminarayanan Mahadevan, Bulbul Chakraborty, and Michael F. Hagan. 2011. Excitable Patterns in Active Nematics. *Physical Review Letters* 106(21): 218101.

Published Version

doi:10.1103/PhysRevLett.106.218101

Permanent link

<http://nrs.harvard.edu/urn-3:HUL.InstRepos:5128482>

Terms of Use

This article was downloaded from Harvard University's DASH repository, and is made available under the terms and conditions applicable to Open Access Policy Articles, as set forth at <http://nrs.harvard.edu/urn-3:HUL.InstRepos:dash.current.terms-of-use#OAP>

Share Your Story

The Harvard community has made this article openly available.
Please share how this access benefits you. [Submit a story](#).

[Accessibility](#)

Excitable Patterns in Active Nematics

L. Giomi,^{1,2} L. Mahadevan,¹ B. Chakraborty,² and M. F. Hagan²

¹*School of Engineering and Applied Sciences, Harvard University, Cambridge, MA 02138, USA*

²*Martin A. Fisher School of Physics, Brandeis University, Waltham, MA 02454, USA*

(Dated: November 18, 2010)

We analyze a model of mutually-propelled filaments suspended in a two-dimensional solvent. The system undergoes a mean-field isotropic-nematic transition for large enough filament concentrations and the nematic order parameter is allowed to vary in space and time. We show that the interplay between non-uniform nematic order, activity and flow results in spatially modulated relaxation oscillations, similar to those seen in excitable media. In this regime the dynamics consists of nearly stationary periods separated by “bursts” of activity in which the system is elastically distorted and solvent is pumped throughout. At even higher activity the dynamics becomes chaotic.

Colonies of motile microorganisms, the cytoskeleton and its components, cells and tissues have much in common with soft condensed matter systems (i.e. liquid crystals, amphiphiles, colloids etc.), but also exhibit phenomena that do not appear in inanimate matter. These unique properties arise when the constituent particles are active: they consume and dissipate energy to fuel internal changes that generally lead to motion. When active particles have elongated shapes, as seen in cytoskeletal filaments and some cells, they undergo orientational ordering at high concentration to form liquid crystalline phases. The theoretical and experimental study of active materials has disclosed a wealth of emergent behaviors, such as the occurrence of *giant* density fluctuations [1], the emergence of spontaneously flowing states (sometimes referred to as flocking) [2], unconventional rheological properties [3] and new spatiotemporal patterns not seen in passive complex fluids [4]. Recently Schaller *et al.* [5] observed collective motion, large-scale fluctuations in density and the degree of polar order, and swirling motions in a motility assay consisting of highly concentrated actin filaments propelled by immobilized molecular motors in a planar geometry. However, the range of behaviors realizable in active materials and the connection between material characteristics and system dynamics remain incompletely understood. In this letter, we show that active systems exhibit behaviors similar to those of excitable systems, showing relaxation oscillations that couple activity to spontaneous pulsatile flow with quiescent periods in between, similar to biological pumps. We furthermore show that systems which undergo nematic ordering can give rise to large-scale swirling motions resembling those observed in Ref. [5] even in the absence of polar order. These behaviors were not seen in previous investigations because they arise only when the degree of nematic order is allowed to fluctuate in space and time.

Our model consists of mutually-propelled elongated particles suspended in a solvent confined to two dimensions, as seen for example in recent motor-filament assays [5]. The dynamical variables in such a system are particle concentrations c , the solvent flow field \mathbf{v} and the nematic tensor $Q_{ij} = S(n_i n_j - \frac{1}{2} \delta_{ij})$, with S the nematic

order parameter and \mathbf{n} the director field, all of which are allowed to vary in space and time. We assume that the suspension of rod-like active particles have length ℓ and mass M in a solvent of density ρ_{solvent} . The total density of the system $\rho = Mc + \rho_{\text{solvent}}$ is conserved, so the fluid is assumed to be incompressible. The total number of active particles is also constant, thus the concentration c obeys the continuity equation:

$$\partial_t c = -\nabla \cdot (\mathbf{j}^p + \mathbf{j}^a), \quad (1)$$

where \mathbf{j}^p and \mathbf{j}^a are respectively the passive and active contributions to the current density. The passive current density has the standard form $j_i^p = cv_i - D_{ij} \partial_j c$ where $D_{ij} = D_0 \delta_{ij} + D_1 Q_{ij}$ is the anisotropic diffusion tensor, while the active current can be constructed phenomenologically to be of the form $j_i^a = -\alpha_1 c^2 \partial_j Q_{ij}$ or derived from microscopic models [6]. Here the factor c^2 reflects the fact that activity arises from interactions between pairs of rods while the constant α_1 describes the level of activity and is proportional to the concentration of motors and the rate of adenosine-triphosphate (ATP) consumption.

The flow velocity obeys an active form of the Navier-Stokes equation

$$\rho \partial_t v_i = \eta \Delta v_i - \partial_i p + \partial_j \tau_{ij}, \quad (2)$$

with η the viscosity, p the pressure, and the active stress tensor τ_{ij} given by:

$$\tau_{ij} = -\lambda S H_{ij} + Q_{ik} H_{kj} - H_{ik} Q_{kj} + \alpha_2 c^2 Q_{ij} \quad (3)$$

Here $\nabla \cdot \mathbf{v} = 0$, and the first three terms in Eq. (3) represent the elastic stress due to the liquid crystalline nature of the system, with $H_{ij} = -\delta F / \delta Q_{ij}$ the molecular tensor defined from the two-dimensional Landau-De Gennes free energy:

$$F/K = \int dA \left[\frac{1}{2} (\nabla \cdot \mathbf{Q})^2 + \frac{1}{4} (c^* - c) \text{tr} \mathbf{Q}^2 + \frac{1}{4} c (\text{tr} \mathbf{Q}^2)^2 \right]$$

where K is the splay and bending stiffness in the one-constant approximation. At equilibrium, above the crit-

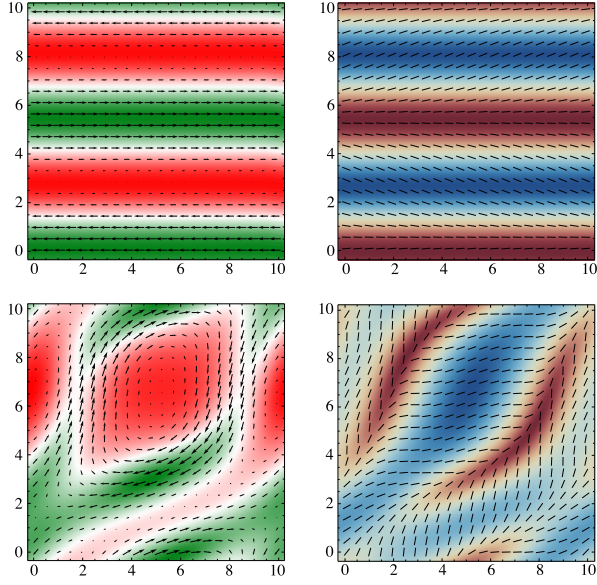


FIG. 1: (Color online) The velocity field (left) and the director field (right) superimposed to a density plot of the concentration and the nematic order parameter for $\alpha_2 = 0.4$ (top) and $\alpha_2 = 3$ (bottom). The colors indicate regions of large (green) and small (red) density and large (blue) and small (brown) nematic order parameter. For moderate values of α_2 the flow consists of two bands traveling in opposite directions with the director field is nearly uniform inside each band. For large α_2 the flow is characterized by large vortices that span lengths of the order of the system size and the director field is organized in grains.

ical concentration c^* , $S = \sqrt{2 \text{tr} \mathbf{Q}^2} = \sqrt{1 - c^*/c}$ consistent with hard-rod fluid models where the isotropic-nematic (IN) transition is driven only by the concentration of the nematogens. The last term was first introduced in Ref. [8] and represents the tensile/contractile stress exerted by the active particles in the direction of the director field \mathbf{n} with α_2 a second activity constant.

Finally, the nematic order parameter Q_{ij} satisfies a hydrodynamic equation that can be obtained by constructing all possible traceless-symmetric combinations of the relevant fields, namely the strain-rate tensor $u_{ij} = \frac{1}{2}(\partial_i v_j + \partial_j v_i)$, the vorticity tensor $\omega_{ij} = \frac{1}{2}(\partial_i v_j - \partial_j v_i)$ and the molecular tensor H_{ij} [7], so that

$$[\partial_t + \mathbf{v} \cdot \nabla] Q_{ij} = \gamma^{-1} H_{ij} + \lambda S u_{ij} + Q_{ik} \omega_{kj} - \omega_{ik} Q_{kj} \quad (4)$$

where γ is an orientational viscosity, and the additional terms on the right-hand side describe the coupling between nematic order and flow in two dimensions, with λ the flow-alignment parameter which dictates how the director field rotates in a shear flow and affects the flow and rheology of active systems [2, 3].

The dynamics of such an active nematic suspension is governed by the interplay between the active forcing, whose rate τ_a^{-1} is proportional to the activity parameters α_1 and α_2 , and the relaxation of the passive structures,

the solvent and the nematic phase, in which energy is dissipated or stored. The response of the passive structures, as described here, occurs at three different time scales: the relaxational time scale of the nematic degrees of freedom $\ell^2/(\gamma^{-1}K)$, the diffusive time scale ℓ^2/D_0 , the dissipation time scale of the solvent $\rho L^2/\eta$, where L is the system size. While the presence of three dimensionless parameters makes for a very rich phenomenology, we temporarily assume that the three passive time scales are of the same magnitude τ_p . When $\tau_a \gg \tau_p$, the active forcing is irrelevant and the system is just a traditional passive suspension. On the other hand, when $\tau_a \sim \tau_p$, the passive structures can balance the active forcing leading to a stationary regime in which active stresses are accommodated via both elastic distortion and flow. Finally, when $\tau_a \ll \tau_p$ the passive structures will fail to keep up, leading to a dynamical and possibly chaotic interplay between activity, nematic order and flow. In the rest of the paper, we quantify these different regimes. We first make the system dimensionless by scaling all lengths using the rod length ℓ , scaling time with the relaxation time of the director field $\tau_p = \ell^2/(\gamma^{-1}K)$ and scaling stress using the elastic stress $\sigma = K\ell^{-2}$.

We start with a linear stability analysis of the hydrodynamic equations about the homogeneous solution letting $\boldsymbol{\varphi} = \{c, Q_{xx}, Q_{xy}, 2\omega_{xy}\} = \boldsymbol{\varphi}_0 + \delta\boldsymbol{\varphi}(t)$ with $\boldsymbol{\varphi}_0 = \{c_0, S_0/2, 0, 0\}$, and consider solutions with periodic boundary conditions on a square domain of the form $\delta\boldsymbol{\varphi}(\mathbf{x}, t) = \sum_{n=-\infty}^{\infty} \sum_{m=-\infty}^{\infty} \boldsymbol{\varphi}_{nm}(t) \exp[\frac{2\pi i}{L}(nx + my)]$. With this choice the linearized hydrodynamic equations reduce to a set of coupled of linear ordinary differential equations for the Fourier modes $\boldsymbol{\varphi}_{nm}$: $\partial_t \boldsymbol{\varphi}_{nm} = \mathbf{A}_{nm} \boldsymbol{\varphi}_{nm}$. The first mode to become unstable is the transverse excitation $(n, m) = (0, 1)$ associated with the block-diagonal matrix:

$$\mathbf{A}_{01} = \begin{pmatrix} \mathbf{a}_{01} & 0 \\ 0 & \mathbf{b}_{01} \end{pmatrix},$$

where:

$$\mathbf{a}_{01} = \begin{pmatrix} -\frac{2\pi^2}{L^2} (2D_0 - D_1 S_0) & \frac{4\pi^2}{L^2} \alpha_1 c_0^2 \\ \frac{c^*}{4c_0} S_0 & -c_0 S_0^2 - \frac{4\pi^2}{L^2} \end{pmatrix}$$

and:

$$\mathbf{b}_{01} = \begin{pmatrix} -\frac{4\pi^2}{L^2} & \frac{1}{2}(1 - \lambda) S_0 \\ \frac{4\pi^2}{L^2} \alpha_2 c_0^2 - \frac{16\pi^4}{L^4} S_0(1 - \lambda) & -\frac{4\pi^2 \eta}{L^2} \end{pmatrix}.$$

The mechanism that triggers the instability of the homogeneous state relies on the coupling between local orientations and flow embodied in the matrix \mathbf{b}_{01} , whose diagonalization yields a lower critical value of α_2 :

$$\alpha_2^* = \frac{4\pi^2 [2\eta + S_0^2(1 - \lambda)^2]}{c_0^2 L^2 S_0(1 - \lambda)}. \quad (5)$$

We see that the critical value of the activity required for instability falls with increasing system size and increases

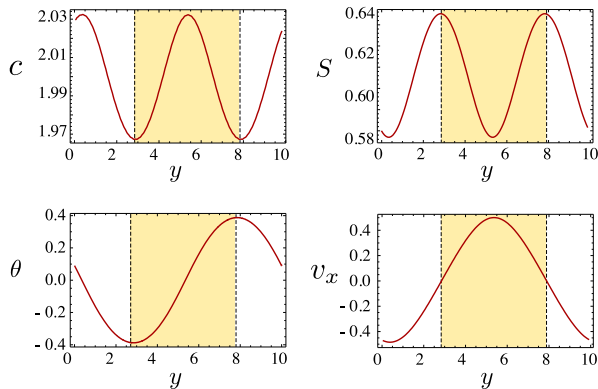


FIG. 2: (Color online) The hydrodynamic fields c , S , θ and v_x along the y axis for $\alpha_2 = 0.4$. The yellow region indicates the band visible in the top panels of Fig. 1.

with the viscosity of the solvent. In general, shear flow causes the director field to rotate for $\lambda \neq 1$, which generates elastic stress. For small activity, the elastic stiffness dominates and suppresses flow, while above α_2^* we observe collective motion.

To go beyond this simple analysis, we numerically integrated the hydrodynamic equations on a two-dimensional periodic domain with initial configurations of a homogeneous system whose director field was aligned along the x axis subject to a small random perturbation in density and orientation, with $\alpha_1 = \alpha_2/2$, $\eta = c^* = D_0 = D_1 = 1$, $\lambda = 0.1$ and $L = 10$. As predicted by the linear stability analysis, at low activity the system relaxes to a stationary homogeneous state with $v_x = v_y = 0$ and $S = \sqrt{1 - c^*/c}$. Above the critical value α_2^* , the system forms two bands flowing in opposite directions. The solution is constant along the flow direction (see Fig. 1 top) while the direction of the streamlines (in this case along the x direction) is dictated by the initial conditions. As shown in Fig. 2, the optima in the flow velocity correspond to the maximal distortion of the director field \mathbf{n} . Variations in concentration c and the nematic order parameter S are of order 2% with a minimum in S at the center of a flowing band due to the balance between diffusive and active currents. We note that these density modulations parallel to the nematic director are characteristic of systems with nematic order, while the density bands orthogonal to the direction of alignment observed in Ref. [5] are consistent with polar order [2].

Upon increasing the value of the activity parameter α_2 , the spontaneously flowing state evolves into a pulsatile spatial relaxation oscillator. Fig. 3 (top left panel) shows a plot of the x and y component of the flow velocity in the center of the box for $\alpha_2 = 1.5$. In this regime the dynamics consists of a sequence of almost stationary passive periods separated by active “bursts” in which the director switches abruptly between two orientations. During passive periods, c and S are nearly uniform, there

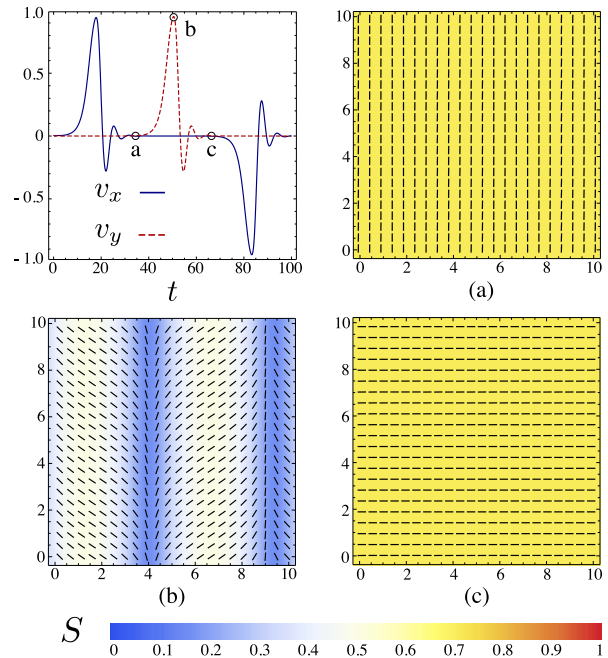


FIG. 3: (Color online) Dynamics of active “burst” for $\alpha_2 = 1.5$. The flow velocity at the point $x = y = L/3$ is shown as a function of time over the course of a director field rotation (top left) and the director field is shown for the three labeled time points. Between two consecutive bursts the system is homogeneous and uniformly aligned. During a burst, nematic order is drastically reduced in the whole system and the director undergoes a distortion with a consequent formation of two bands flowing in opposite directions. After a burst, a stationary state is restored with the director field rotated of 90° with respect to its previous orientation.

is virtually no flow and the director field is either parallel or perpendicular to the x direction. Eventually this configuration breaks down and the director field rotates by 90° (see Fig. 3). The rotation of the director field is initially localized along lines, generating a band of flow similar to those in Fig. 1 (top). The flow terminates after the director field rotates and a uniform orientation is restored. The process then repeats.

This rotation of the director field occurs through a temporary “melting” of the nematic phase. As shown in Fig. 3, during each passive period the nematic order parameter is equal to its equilibrium value $S_0 = \sqrt{1 - c^*/c}$, but drops to $\sim \frac{2}{5}S_0$ during rotation. The reduction of order is system-wide, but, as shown in the middle in the bottom-left panel of Fig. 3, is most pronounced along the boundaries between bands. Without transient melting, the distortions of the director field required for a burst are unfavorable for any level of activity.

To illustrate the origin of the relaxation oscillations it is useful to construct a simplified version of the hydrodynamic equations by retaining the minimal features responsible for the oscillatory phenomenon: the coupling between active forcing and the fluid microstructure and

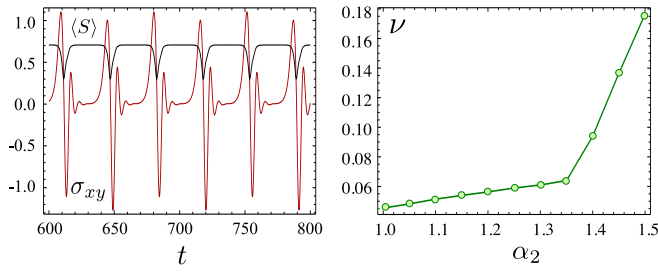


FIG. 4: (Color online) (Left) The average nematic order parameter $\langle S \rangle$ and the total shear stress σ_{xy} are shown over several bursts for $\alpha_2 = 1.5$. (right) The frequency of bursts is shown as a function of α_2 .

the variable nematic order embedded in the Landau-De Gennes free energy. This can be achieved by approximating Q_{xx}^2 as a constant and $u_{xx} \approx 0$. Then, letting $u = -u_{xy}$ and $Q = Q_{xy}$, and dropping the coupling between Q_{ij} and ω_{ij} , Eqs. (2) and (4) can be expressed in Fourier space as:

$$\dot{Q} = aQ - bQ^3 - u \quad (6a)$$

$$\dot{u} = k^2(\alpha Q - u) \quad (6b)$$

where k is a wave number of an arbitrary spatial mode and a and b are constants. Eqs. (6) has the form of the FitzHugh-Nagumo model for excitable dynamical systems. For $\alpha < \frac{1}{3}(2a + k^2)$ the system rapidly relaxes to a state characterized by a finite strain-rate that balances the active stress: $u = \alpha Q = \alpha\sqrt{(a - \alpha)/b}$. For $\alpha > \frac{1}{3}(2a + k^2)$, this state becomes unstable and the trajectory converges to a limit cycle with a frequency $\nu \sim k^2\alpha$. As anticipated, when the active and passive time-scales are comparable the active forcing is accommodated by the microstructure leading to a distortion of the director field and a steady flow. However, when the active forcing rate is increased, the microstructure dynamics lag, resulting in oscillatory dynamics. Clearly, the full system exhibits a much richer behavior than that captured by Eqs. (6), but the qualitative trends persist. For instance, the increase in the slope of ν shown in Fig. 4 is not simply associated with the excitation of a second spatial mode of larger wave-number and is more likely due to the dynamics of the concentration field, which has been ignored in Eqs. (6).

When the activity α_2 is further increased, the sequence of low activity periods and bursts becomes more complex and eventually chaotic. We emphasize that the oscillatory dynamics and the chaotic flows discussed below do not occur in our equations unless the magnitude of the nematic order parameter is allowed to fluctuate. Fig. 1 (bottom) shows a typical snapshot of the flow velocity and the director field superimposed to a density plot of the concentration and the nematic order parameter respectively. The flow is characterized by large vortices with positions related to “grains” in which the director

field is uniformly oriented. The grain boundaries are of the order of the system size and are the fastest flowing regions in the system. Thus the dynamics in this regime is characterized by sets of grains of approximately uniform orientation that swirl around each other and continuously merge and reform.

In summary, we analyzed the hydrodynamics of active nematic suspensions in two dimensions. By allowing spatial and temporal fluctuations in the nematic order parameter we have observed a rich interplay between order, activity and flow. Significantly, we find that allowing fluctuations in the magnitude of the order parameter S qualitatively changes the flow behavior as compared to systems in which S is constrained to be uniform. Finally, we note that both the flip-flop dynamics (Fig. 3) and the swirling motion (Fig. 1 bottom) resemble behavior observed in the motility assay experiments of Schaller *et al.* [5]. Our analysis suggests that these classes of patterns can emerge even in the absence of polar order.

We gratefully acknowledge support from the NSF Brandeis MRSEC (LG, BC, and MFH), the NSF Harvard MRSEC (LG,LM), NIAID R01AI080791 (MFH), the Harvard Kavli Institute for Nanobio Science & Technology (LG, LM), and the MacArthur Foundation (LM).

-
- [1] V. Narayan, S. Ramaswamy and N. Menon, *Science* **317**, 105 (2007). J. Deseigne, O. Dauchot and H. Chaté, *Phys. Rev. Lett.* **105**, 098001 (2010).
 - [2] R. Voituriez, J. F. Joanny and J. Prost, *Europhys. Lett.* **70**, 118102 (2005). D. Marenduzzo, E. Orlandini, M. E. Cates, and J. M. Yeomans, *Phys. Rev. E* **76**, 031921 (2007). L. Giomi, M. C. Marchetti and T. B. Liverpool, *Phys. Rev. Lett.* **101**, 198101 (2008). S. Mishra, A. Baskaran and M. C. Marchetti, *Phys. Rev. E* **81**, 061916 (2010).
 - [3] M. E. Cates, S. M. Fielding, D. Marenduzzo, E. Orlandini and J. M. Yeomans, *Phys. Rev. Lett.* **101**, 068102 (2008). A. Sokolov and I. S. Aranson, *Phys. Rev. Lett.* **103**, 148101 (2009). L. Giomi, T. B. Liverpool and M. C. Marchetti, *Phys. Rev. E* **81**, 051908 (2010). D. Saintillan, *Phys. Rev. E* **81**, 056307 (2010).
 - [4] D. Saintillan and M. J. Shelley, *Phys. Rev. Lett.* **100**, 178103 (2008). H. Chaté, F. Ginelli and R. Montagne, *Phys. Rev. Lett.* **96**, 180602 (2006). F. Ginelli *et al.* *Phys. Rev. Lett.* **104**, 184502 (2010).
 - [5] V. Schaller, C. Weber, C. Semmrich, E. Frey and A. R. Bausch, *Nature* **467**, 73 (2010).
 - [6] A. Ahmadi, M. C. Marchetti and T. B. Liverpool, *Phys. Rev. E* **74**, 061913 (2006). T. B. Liverpool and M. C. Marchetti, *Hydrodynamics and rheology of active polar filaments*, in *Cell Motility*, P. Lenz ed. (Springer, New York, 2007).
 - [7] P. D. Olmsted and P. M. Goldbart, *Phys. Rev. A* **46**, 4966 (1992).
 - [8] T. J. Pedley and J. O. Kessler, *Annu. Rev. Fluid Mech.* **24**, 313 (1992).